

CHEMICAL LEACHING OF Al_3Ni AND Al_3Ti ALLOYS
AT ROOM TEMPERATUREIvan Saldan¹, L'ubomir Orovčik², Oksana Dobrovetska³, Oleh Bilan⁴, Orest Kunttyi³, ✉<https://doi.org/10.23939/chcht15.01.081>

Abstract. Al_3Ni and Al_3Ti alloys were prepared by arc melting and exposed to chemical leaching in 5M NaOH at room temperature. In case of Al_3Ni alloy, Al reached phases react with the leaching solution to produce nanoporous nickel with a pore diameter in the range of ~10–20 nm. Only pure Al phase of Al_3Ti alloy chemically reacts with the production of a dense wrinkled surface with a wrinkle size of ~50–100 nm.

Keywords: nickel, titanium, porous material, X-ray diffraction, surface morphology.

1. Introduction

High efficiency of micro- and nanoporous materials in catalysis, sensors, water purification, energy storage, *etc.*, revealed a great interest to their study in the last decade [1-10]. They can be made of carbon materials [3], pure metals [4-6], metal oxides [5], semiconductors [6, 7], hybrid composites including natural aluminosilicates [9] and polymers [10]. Spongy metals (*e.g.* nickel and titanium) in terms of cost and simple way of production are very promising porous materials well known as catalysts in many chemical reactions. Since the main properties of such materials determined by the porosity architecture and the geometry of its fragments, the method of preparation plays the most responsible role in the connection of four units:

“method→structure→properties→application”.

Today, in term of macroporous materials (particle size of 50–1000 nm) nickel and titanium sponges do not meet the modern requirements of nanotechnologies where surface effects started to dominate in micropores (size of

0.2–2 nm). Therefore preparation of the microporous materials, mainly used as solid nanocatalysts, is a topical task. Moreover, when a specific method to form this porous structure allows to control surface properties, it is a good opportunity to predict kinetics and even reaction mechanism. The preparation of the microporous materials based on nickel and titanium needs to be further developed. High level technologies require a simple preparation method with a definite chemical composition (*e.g.* pure metals, metal oxides or even layered metal/oxide structure). In addition, the preparation of microporous materials needs to be a convenient and not expensive technology in practice. Chemical and electrochemical leaching of alloys that contains active component selectively dissolved in a certain solution may result in de-alloying to form 3D porous structure (Table 1) [11].

In a typical de-alloying procedure, a surface alloy (made of *e.g.* intermetallic compounds and/or solid solutions) comes in contact with an electrolyte solution and the less noble component is electrochemically dissolved, while the atoms of noble component rearrange on the alloy surface resulting in a porous 3D structure. The driving force for the de-alloying is that the alloy components should have a substantial difference in their standard redox potentials [1, 24]. In work [24] a continuum model of alloy dissolution demonstrates that nanoporosity in metals is due to an intrinsic dynamical pattern formation process. The main reason of pore formation is the situation when more noble atoms are chemically driven to aggregate into two-dimensional clusters by a phase separation process at the solid/ electrolyte interface. Thus, the surface area continuously increases owing to electrochemical dissolution. A schematic illustration of how porosity evolves during de-alloying of Al from Al-Ni alloys was shown recently [12]. At the first step, the surface of the Ni-Al alloys is exposed with regions of accumulated noble component (Ni) at the base of the already-formed nanoporous skeleton. Atoms of the less noble component (Al) in the exposed alloy surface are dissolved into the electrolyte. At the second stage, the surface area increases with increasing interfaces during dissolving at the first step and the noble Ni

¹ Ivan Franko National University of Lviv,
6, Kyryla & Mefodia St., Lviv, 79005, Ukraine

² Institute of Materials & Machine Mechanics, Slovak Academy of Sciences,

9, Dúbravská cesta, 84513 Bratislava, Slovakia

³ Lviv Polytechnic National University,
12, S. Bandery St., Lviv, 79013, Ukraine

⁴ Industrial Company “Autonomous Power Sources”,

2, Lvivska St., Velyki Mosty 80074, Ukraine

✉ kunttyi@ukr.net

© Saldan I., Orovčik L., Dobrovetska O., Bilan O., Kunttyi O., 2021

adatoms are released onto the surface. These Ni adatoms are collected onto already-agglomerated Ni atom clusters, or nucleate new clusters when Ni atom ligaments are too far away. At the final stage, the less noble element (Al) in the Ni-Al alloy surface dissolves into the electrolyte; Ni agglomeration repeats and pore surface area increases. In practice, de-alloying approach of Al-Ni alloys [14] has been proposed to create porous Ni-based materials. Using hydrogen plasma-metal reaction and chemical leaching with a simple passivation process, nanoparticles with a Ni@NiO structure were successfully formed. They were recommended as an electrode material for supercapacitors since they have exhibited specific capacitance value of ≈ 640 F/g at 1 A/g [14]. Another example – a macroporous TiO₂ network was formed on the surface of Al-Ti alloys through a chemical de-alloying [25]. The TiO₂ film obtained exhibited a high surface hydrophilic

activity and light absorbance, hence it might be recommended for photochemical reactions.

The main purpose of the present experimental work is the preparation of a porous solid structure through the chemical leaching of Al based alloys. In order to develop chemical de-alloying the arc-melted Al₃Ni and Al₃Ti alloys were leached in 5M NaOH at room temperature during 4 and 8 days and tested afterwards. Detailed characterization of the prepared and leached samples was made using a powder X-ray diffraction (XRD) and a scanning electron microscopy with energy dispersive X-rays (SEM-EDX). Proposed chemical de-alloying might be used as a selective chemical leaching to obtain porous materials with a special nano-design. From practical point of view, prepared porous materials might be recommended as novel electrodes in batteries and capacitors [26, 27], effective catalysts in chemical reactions and nano-scaffolds for solution impregnation [28] or melt infiltration processes [29].

Table 1

Precursors and chemical composition of the leaching solution to obtain nickel or titanium sponges using a selective dissolution of binary M-Ni and M-Ti systems (M is a chemically active component)

Precursor	Leaching solutions or electrolyte with potentials values	Average pore diameter	Ref.
Ni ₃₀ Al ₇₀ Ni ₅₀ Al ₅₀	1M NaOH at $E \geq -0.3$ V	71.10 ± 43.69 nm 40.84 ± 24.70 nm	[12]
Ni ₂₀ Al ₈₀	2M NaOH	70 ± 19 nm	[13]
Al ₃ Ni ₂ nanoparticles	5M NaOH	Nanoporous Ni nanorarticles	[14]
Ni ₃₀ Mn ₇₀	1M (NH ₄) ₂ SO ₄ at $E = -0.65$ V	~10 nm	[15]
Ni ₃₈ Mn ₆₂	NH ₄ H ₂ PO ₄ at $E = -0.3$ V; 0.45 V	150–440 nm or 70–130 nm	[16]
Ni ₃₀ Mn ₇₀	1M (NH ₄) ₂ SO ₄ at 323–343 K or $E = (-0.75)–(-0.45)$ V	~6 nm	[17]
Ni ₃₃ Cu ₆₇ Ni _{25–35} Al _{65–75} Ni ₃₀ Fe ₇₀ Ni ₃₃ Mg ₆₇	1NH ₃ :H ₂ O :1H ₂ O ₂ , 323 K 1NH ₃ :H ₂ O :1H ₂ O ₂ , 293 K H ₃ PO ₄ HAc	~8 nm ~4 nm ~12 nm ~7 nm	[18]
Ni-Cu	0.5M H ₃ BO ₃ + 0.5M Na ₂ SO ₄ at ($E_1 = 0.5$, $E_2 = 0.07$ V in pulse regime)	100–300 nm	[19]
Ni-WC	1.5M NaOH at $E = 1.5$ V	1 ± 0.5 μm	[20]
Mg-Ti	2M HCl	132–262 μm	[21]
Ti-Sc	HNO ₃ (70%)	~100 nm	[22]
Ti-Cu	Mg powders at 773–873 K, after etched by 1M HNO ₃	2–50 nm	[23]

2. Experimental

2.1. Alloy Preparation

The composition of Al₃Ni and Al₃Ti alloys was selected as starting aluminum alloys from the binary metallic system Al-Ni and Al-Ti [11, 12]. The alloys ingots were prepared by arc melting of stoichiometric amount of aluminum (99.99 %, Stanford Materials Corporation) with nickel or titanium (99.995 %, Kurt J. Lesker Company). It was performed in the arc furnace (CENTORR Vacuum Industries) equipped with a tungsten

electrode and a water-cool copper plate upon which the metal pieces were placed. Pure argon was used both for protective atmosphere and for the production of current carrying plasma. Upon the synthesis of samples, a titanium getter was first melted to avoid oxygen contamination on the samples which were melted after and then turned upside down to be re-melted five times to ensure maximum homogeneity. Prepared alloys were cut using Leihmaschine (BUEHLER) instrument equipped with an abrasive cut-off wheel for non-ferrous materials and water flow. The alloy plates (~6×6 mm in size and ~0.2–0.6 mm in thickness) were ultra-sonicated and dried

in air. Obtained alloy plates were immersed in 5M NaOH for 4 and 8 days at room temperature. Prepared and leached samples were rinsed with distilled water and used for XRD and SEM-EDX analysis.

2.2. X-ray Diffraction Analysis

XRD was performed in a Bruker AXS D8 Advance instrument with a LynxEye™ XE position sensitive detector using Cu K_α radiation. Obtained Al₃Ni and Al₃Ti plates after preparation and chemical leaching were attached to the XRD sample holder by a sticking tape. Data acquisition was performed with a step size of 0.02 and 2s/step measurement time within the range of 2θ = 10–100°. The Bruker-AXS software EVA coupled with the PDF-4 structure database was used for phase identification.

2.3. Scanning Electron Microscopy Measurements

Morphology of the prepared and leached Al₃Ni and Al₃Ti plates was studied using a Field Emission Scanning Electron Microscopy (FE-SEM). Micrographs were obtained using a scanning electron microscope (JEOL JSM-7600F) which features a high brightness Schottky field emission source and an in-lens secondary electron detector. The samples were mounted directly on a standard aluminum stub using a bi-adhesive conductive tape. All SEM-EDX measurements were performed on the alloy surface with the acceleration potential of 5 kV at the working distance of approximately 5 mm. SEM images were prepared with the magnification of 50,000 and 150,000 times. The chemical composition of the prepared Al₃Ni and Al₃Ti alloys was determined through EDX analysis using a detector (Oxford Instruments, X-max 50 mm² Tokyo, Japan) directly coupled with FE-SEM as in [13]. For EDX microanalysis the alloy plates were first polished on SiC emery paper (up to 1000 mesh) and afterwards with a diamond suspension (6, 3 and 1 μm grain size). Then all samples were ultrasonicated in a water bath for 20 min.

3. Results and Discussion

3.1. Phase Analysis of the Prepared and Leached Alloys

Powder XRD results for the prepared Al₃Ni alloy and after 4 or 8 days of its chemical leaching in 5M NaOH at room temperature are shown in Fig. 1. Diffraction pattern for the prepared alloy (Fig. 1a) confirmed multi-phase material with pure Al (*face-centered*

cubic system), and two intermetallic compounds – Al₃Ni (orthorhombic symmetry, *Pnma*) and Al₃Ni₂ (trigonal symmetry, *P3-*m*1*). It should be mentioned that there were no diffraction peaks attributed to a Ni based phase in the prepared Al₃Ni alloy, while after a 4-day leaching procedure all Al-based phases vanished away and wide peaks of pure Ni (cubic symmetry, *Fm3-*m**) appeared (Fig. 1b). During further chemical leaching XRD analysis suggested appearance of a new phase – NiO (cubic symmetry, *Fm3-*m**) (Fig. 1c). For both leached samples SiO₂ (monoclinic symmetry, *C2/**m*) an additive was found and was considered as an impurity because of the procedure of cutting using the abrasive cut-off wheel made of SiC and SiO₂. Most probably, SiO₂ pieces struck on the cutting surface of the Al₃Ni alloy and finally got attached to the rough alloy plate. Therefore, they are almost not visible for the prepared Al₃Ni alloy among Al-reached phases, while diffraction peaks of crystalline SiO₂ became easily identified together with nanostructured Ni/NiO (Fig. 1b, c).

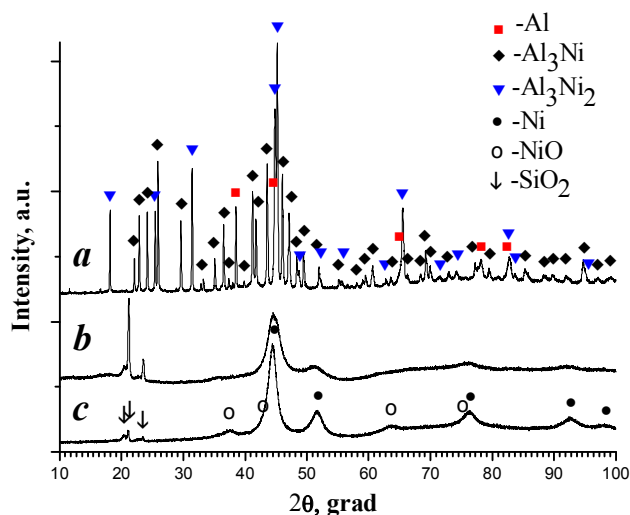
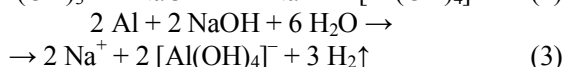
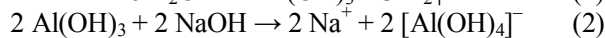


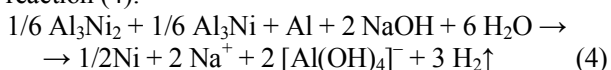
Fig. 1. XRD patterns for the prepared Al₃Ni alloy (a) and after 4- (b), 8 (c) days of its chemical leaching in 5M NaOH at room temperature

Taking into account *ex situ* XRD results obtained for the Al₃Ni alloy during the chemical leaching process, a hypothetical reaction mechanism might be proposed [4]:



It is well known that because of an impermeable protective layer composed of aluminum hydroxide pure aluminum does not react with water under ambient conditions. The formation of the protective layer is prevented with the addition of sodium hydroxide which is

introduced in the solution with the production of aluminates. According to the experimental work [4], Al atoms in the Ni-Al intermetallic compounds might be continuously dissolved into the solution while Ni atoms remain stable during chemical dealloying. In our case, since three Al-based compounds can react with aqueous solution of NaOH simultaneously to produce pure Ni and water-soluble $\text{Na}[\text{Al}(\text{OH})_4]$, they might be combined in the reaction (4):



The metallic nickel obtained, especially in a nano-structured shape, might be oxidized at room temperature to form stable nickel(II) oxide on the solid surface. In practice, chemical leaching for the prepared Al_3Ni alloy was accompanied by intensive gassing that might be accounted for by a hydrogen gas evolution during (1, 3, 4) chemical reactions. Permanent hydrogen gas evolution might promote the formation of a porous structure through the bulk of the Al_3Ni alloy and thus porous material made of pure nickel can be prepared. However, at the contact of the solid surface with the leaching solution an oxidation reaction also takes place at room temperature to oxidize metallic nickel to NiO.

Similar powder XRD measurements were carried out for Al_3Ti alloy after its preparation and chemical leaching (Figs. 2 and 3). At the first glance the diffraction pattern for the prepared alloy (Fig. 2a) suggested the main Al_3Ti (tetragonal symmetry, $I4/mmm$) phase with the secondary SiO_2 (monoclinic symmetry, $C2/m$), TiO (monoclinic symmetry, $A2/m$), and pure Al (fcc) (Fig. 2a). However, a detailed XRD analysis (Fig. 3) also revealed $\text{Al}_{2.92}\text{Si}_{0.08}\text{Ti}$ phase with the same crystal structure but higher values of cell parameters than those for Al_3Ti

because of visible diffraction peak shift to lower 2θ . Appearance of $\text{Al}_{2.92}\text{Si}_{0.08}\text{Ti}$ in prepared Al_3Ti alloy was rather the result of an impurity in the parent mixture before arc melting than Al_3Ti contact with abrasive cut-off wheels (because of Si or SiC). XRD experiments confirmed that obtained alloy plates were contaminated deeper by SiO_2 and titanium(II) oxide was a product of Al_3Ti alloy preparation (not chemical leaching). As compared to XRD patterns of the prepared Al_3Ti alloy, those of the leached samples changed not so much (Fig. 2b, c). After a 4-day leaching procedure the pure Al phase disappeared superficially while the Al_3Ti phase still remained (Fig. 2b).

XRD pattern for the sample after 8 days of leaching confirmed the same phase existence as that after 4 days of leaching. After chemical leaching a strong intensity increase only for the diffraction peaks at $2\theta \sim 39^\circ$ and $\sim 75^\circ$ suggested respectively two main crystallographic directions (112) and (116) on the solid surface (Fig. 2b, c). This fact means that Al_3Ti phase did not react chemically with the leaching solution. Because of pure Al extraction on the surface of the prepared Al_3Ti alloy, intermetallic compound Al_3Ti compacted mainly in (112) and (116) directions (Fig. 2c). Chemical leaching for the prepared Al_3Ti alloy was also accompanied by a gas evolution. Most probably in this case the reaction (1) also took place but only on the surface since it was not so intense as that for Al_3Ni alloy. This situation suggested prevalence of diffusion model of chemical leaching since reactants delivery and removal of reaction products might be the slowest stages. However, when the chemical interaction between Al_3Ti and NaOH takes place, similar chemical leaching mechanism as in case of the Al_3Ni alloy is considered.

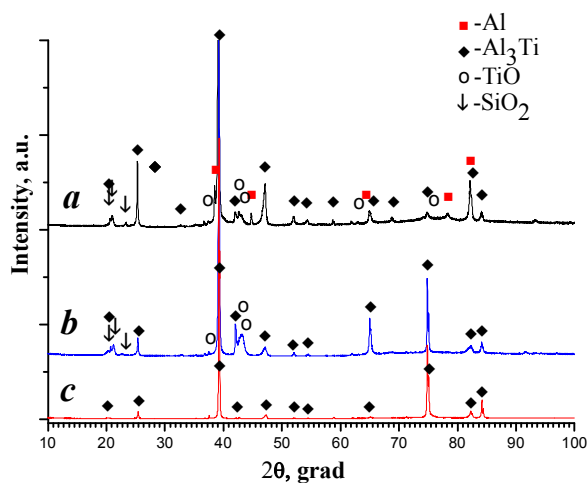


Fig. 2. XRD patterns for the prepared Al_3Ti alloy (a) and after 4 (b), 8 (c) days of its chemical leaching in 5M NaOH at room temperature

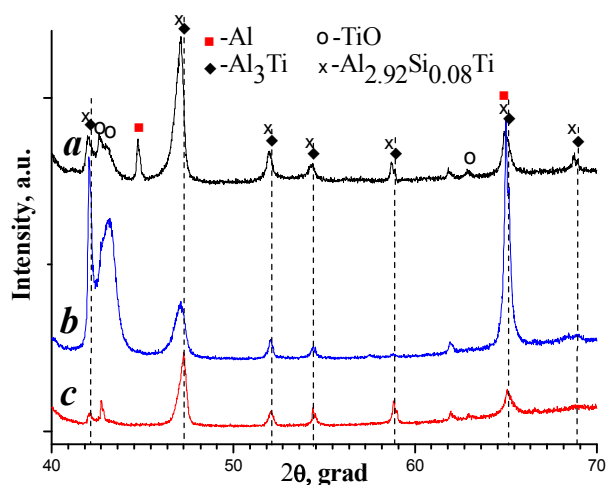


Fig. 3. XRD patterns within the short range of 2θ for the prepared Al_3Ti alloy (a) and after 4 (b), 8 (c) days of its chemical leaching in 5M NaOH at room temperature

3.2. Surface Morphology and Energy Dispersive X-ray Analysis

SEM-EDX experiments carried out for the prepared Al_3Ni alloy (Fig. 4a) correlated well with XRD results (Fig. 2a). Phase approximation based on EDX data suggested two intermetallic compounds (Al_3Ni and

Al_3Ni_2) and two solid solutions (Ni in Al [7] and Ni with W in Al) (Table 2). Most probably, Ni additive was obtained during arc melting of the parent mixture and W could be considered as the impurity from a tungsten electrode. Since the cutting surface of Al_3Ni plates was mechanically removed by polishing, no SiO_2 impurity was found.

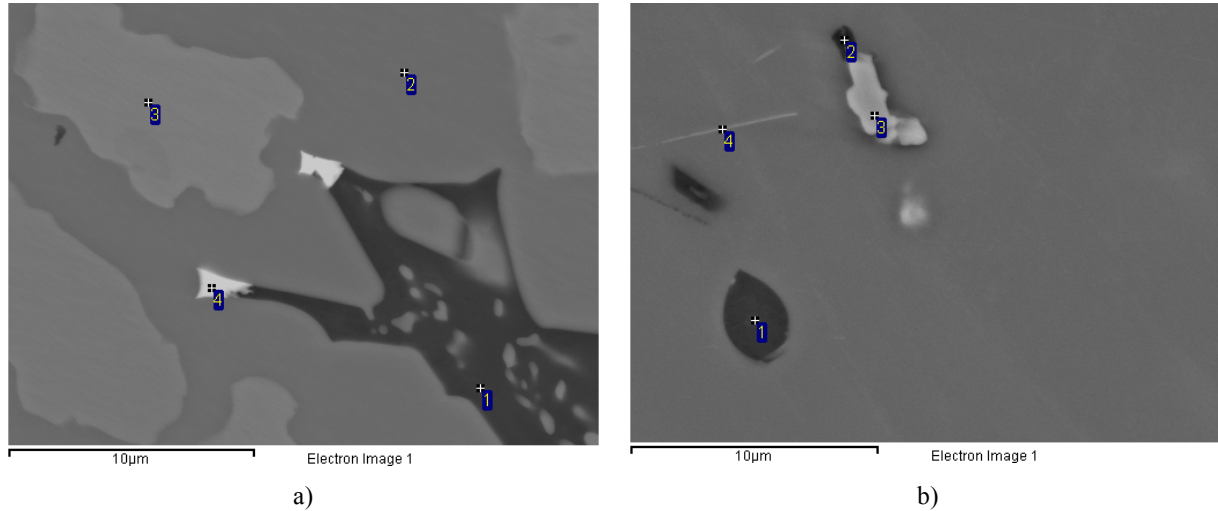
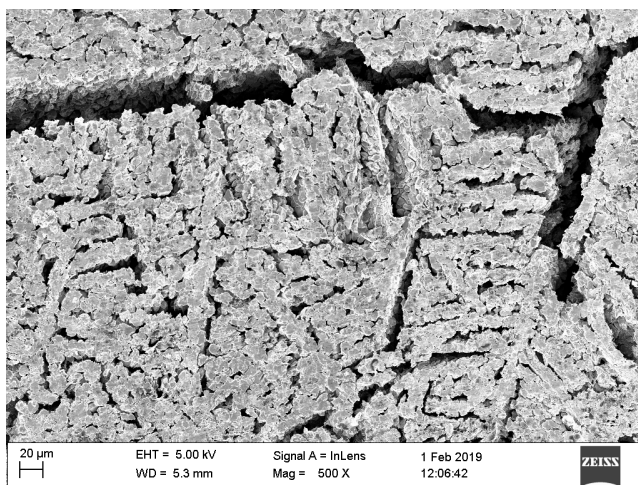


Fig. 4. SEM image for the polished surface of the prepared Al_3Ni (a) and Al_3Ti (b) alloy

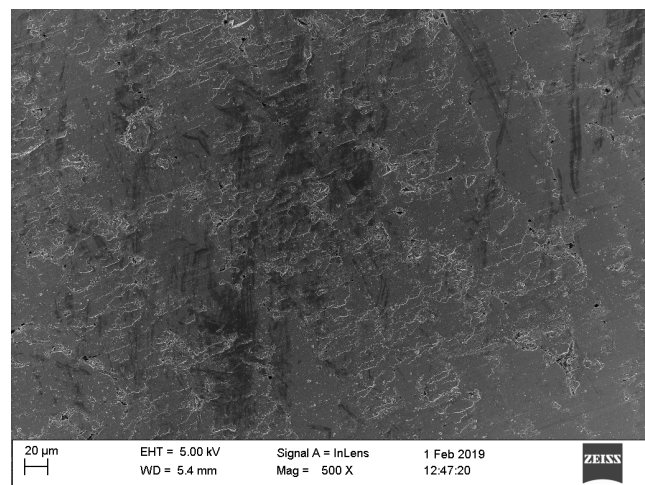
Table 2

EDX results for the surface of the prepared Al_3Ni alloy

Position number	Al, at. %	Ni, at. %	W at. %	Phase approximation
1	98.42	1.58	—	Solid solution of Ni in Al
2	75.38	24.62	—	Al_3Ni
3	61.96	38.04	—	Al_3Ni_2
4	77.28	9.15	13.58	Solid solution of Ni and W in Al



a)

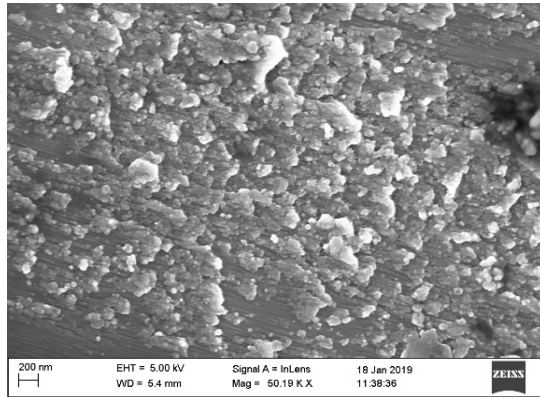


b)

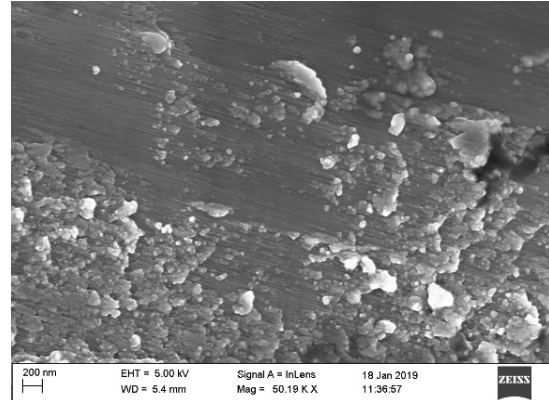
Fig. 5. SEM images for the surface of Al_3Ni (a) and Al_3Ti (b) alloy after 8 days of its chemical leaching in 5M NaOH at room temperature

EDX results for the surface of the prepared Al_3Ti alloy

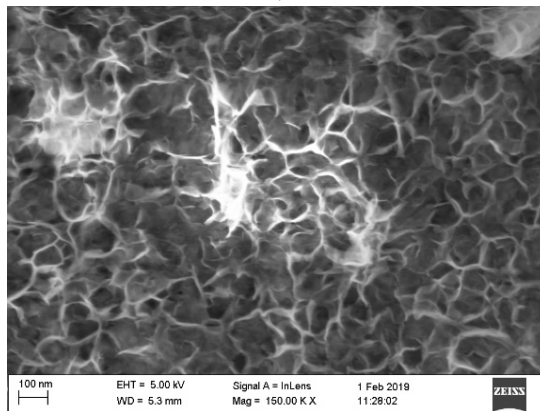
Position number	Al, at. %	Ti, at. %	Si at. %	Phase approximation
1	98.54	1.46	—	Solid solution of Ti in Al
2	84.46	15.54	—	Solid solution of Ti in Al
3	10.08	89.92	—	Solid solution of Al in Ti
4	73.96	24.89	1.15	$\text{Al}_{2.97}\text{Si}_{0.05}\text{Ti}$



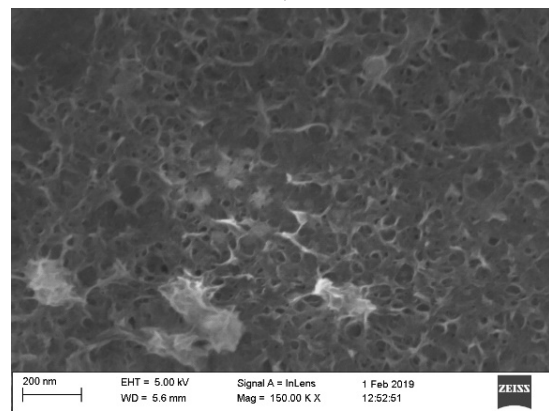
a)



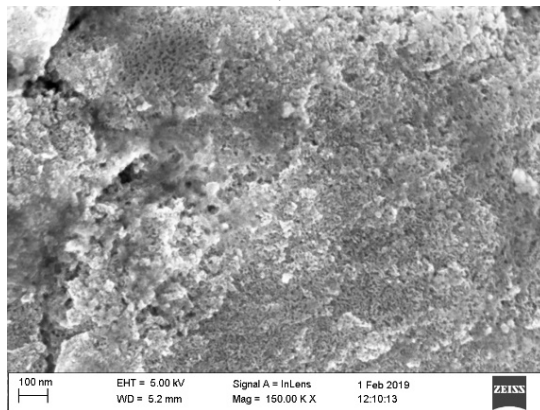
b)



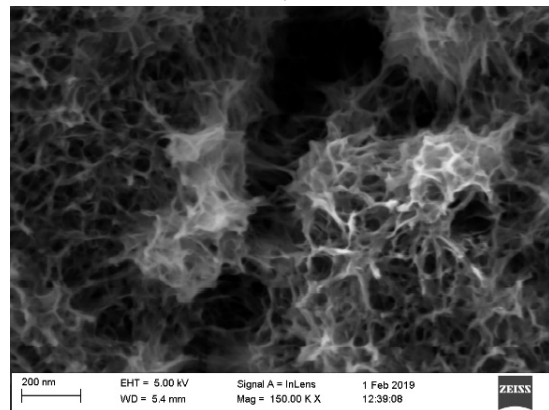
c)



d)



e)



f)

Fig. 6. SEM images for the surface of Al_3Ni and Al_3Ti alloys as prepared (a, b), after 4 (c, d) and 8 days (e, f) of its chemical leaching in 5M NaOH at room temperature, respectively

For the prepared Al₃Ti alloy SEM-EDX results (Fig. 4b) suggested both Al₃Ti and Al_{2.92}Si_{0.08}Ti as the total Al_{2.97}Si_{0.05}Ti phase approximation (Table 3). It looked like they formed the basis with two solid solutions (Ti in Al and Al in Ti [8]). Most probably, both solid solutions were obtained during arc melting of the parent mixture. And XRD conclusions on the appearance of the TiO phase in the prepared alloy might be related to a solid solution of Al in Ti that was oxidized on the surface. Similar to the prepared Al₃Ni alloy, SiO₂ impurity was not identified by SEM-EDX.

Morphology of the Al₃Ni and Al₃Ti alloy after 8 days of chemical leaching in 5M NaOH at room temperature showed a huge difference even at low magnification (Fig. 5). Surface of Al₃Ni alloy was totally cracked very deep in the bulk (Fig. 5a) while morphology of the Al₃Ti alloy was almost not changed after applied chemical leaching (Fig. 5b). This was the first direct confirmation that chemical interaction with leaching solution took place only for the prepared Al₃Ni alloy resulting in a complete destruction of solid surface forming clacks in size of some microns. Most probably cracks appearance was promoted by the existence of multiphase composition and in case of single phase a homogeneous porous structure would be prepared.

Higher magnifications for SEM images were used to analyze the whole leaching process. The morphology of the prepared Al₃Ni and Al₃Ti alloys was very similar and reminded a surface with high roughness (Figs. 6a, b). During chemical leaching procedure the surface underwent major changes producing considerable corrugation. After 4 days of chemical leaching in 5M NaOH at room temperature the surface of both alloys got totally covered with wrinkles around ~100 nm long (Figs. 6c, d). It should be mentioned that for the Al₃Ni alloy the wrinkles observed were more homogeneous and denser as compared to those for Al₃Ti. Finally, after 8 days of leaching further corrugation resulted in a nanoporous structure of Al₃Ni alloy and a dense wrinkled surface for Al₃Ti (Fig. 6e, f). Morphology observations directly confirmed that applied chemical leaching stimulated the higher surface roughness with pores diameter of ~10–20 nm deep in case of Al₃Ni alloy or wrinkles of ~50–100 nm on the surface of Al₃Ti alloy.

Since the value of redox potential for Al and Ni is -1.67 and -0.25 V, respectively, their difference is enough to be the driving force for the de-alloying for Al-Ni intermetallic compounds or solid solutions. Proposed chemical de-alloying might be considered as a chemical leaching to obtain porous nickel with a special nano-design. The redox potential value of Ti (-1.63 V) is very similar to that as of Al, therefore de-alloying cannot appear in Al-Ti intermetallic compounds or solid solutions.

4. Conclusions

For the prepared Al₃Ni alloy three phases (Al₃Ni, Al₃Ni₂ and pure Al) were identified by the powder XRD and SEM-EDX experiments. During chemical leaching in 5M NaOH at room temperature all Al based compounds totally vanished, while amorphous Ni appeared. Further leaching procedure resulted in more structured metallic Ni with the surface oxidized to NiO. Because of permanent intense hydrogen gas evolution during leaching the Ni material obtained possessed a porous structure. Applied chemical leaching stimulated a higher surface roughness that might finally produce the bulk pores with the diameter in the range of ~10–20 nm. This engineering approach might be proposed for production of Ni or NiO mesoporous networks to be used as effective catalyst in chemical reactions.

The Al₃Ti alloy prepared is characterized by Al₃Ti and pure Al. Experimental results suggested on the surface interaction with the leaching solution only for pure Al, while Al₃Ti and Al_{2.92}Si_{0.08}Ti phases demonstrated their compactness mainly in (112) and (116) directions. After 8 days of leaching a dense wrinkled surface for Al₃Ti was formed. Morphology observations directly confirmed the development of wrinkles of ~50–100 nm on the alloy surface. Depending on the quantity and distribution of pure Al in Al₃Ti alloy, the chemical interaction between Al and water solution of NaOH will take place to produce a wrinkled alloy surface.

Acknowledgements

Alloy preparation and SEM observations for the alloys after chemical leaching were carried out within the frame of Swedish Institute scholarship (23891/2017) obtained by Dr. I. Saldan, under the supervision of Assoc. Prof. Dr. Martin Häggblad Sahlberg, and assistance of Dr. Eirini-Maria Paschalidou (Ångström, Uppsala University). The authors thank for financial support provided by the Ministry of Education and Science of Ukraine (reference numbers 0117U001235 and 0118U000268).

References

- [1] Xu Q. (Ed.): Nanoporous Materials. Synthesis and Applications. Taylor and Francis Group LLC, London 2013.
- [2] Gao H., Wang J., Chen X. *et al.*: Nano Energy, 2018, **53**, 769. <https://doi.org/10.1016/j.nanoen.2018.09.007>
- [3] Kumar K., Preuss K., Titirici M.-M. *et al.*: Chem. Rev., 2017, **117**, 1796. <https://doi.org/10.1021/acs.chemrev.6b00505>
- [4] Zhu C., Du D., Eychmüller A. *et al.*: Chem. Rev., 2015, **115**, 8896. <https://doi.org/10.1021/acs.chemrev.5b00255>
- [5] Huang A., He Y., Zhou Y. *et al.*: J. Mater. Sci., 2019, **54**, 949. <https://doi.org/10.1007/s10853-018-2961-5>

- [6] Pia G., Brun M., Aymerich F. *et al.*: J. Mater. Sci., 2017, **52**, 1106. <https://doi.org/10.1007/s10853-016-0407-5>
- [7] Zuo X., Zhu J., Müller-Buschbaum P. *et al.*: Nano Energy, 2017, **31**, 113. <https://doi.org/10.1016/j.nanoen.2016.11.013>
- [8] Shepida M., Kuntiyi O., Nichkalo S. *et al.*: Adv. Mater. Sci. Eng., 2019, **2019**. <https://doi.org/10.1155/2019/2629464>
- [9] Wafiroh S., Abdulloh A., Widati A.: Chem. Chem. Technol., 2018, **12**, 229. <https://doi.org/10.23939/chcht12.02.229>
- [10] Saldan I., Stetsiv Y., Makogon V., *et al.*: Chem. Chem. Technol., 2019, **13**, 85. <https://doi.org/10.23939/chcht13.01.085>
- [11] McCue I., Benn E., Gaskey B. *et al.*: Ann. Rev. Mater. Res., 2016, **46**, 263. <https://doi.org/10.1146/annurev-matsci-070115-031739>
- [12] Rahman Md.A., Zhu X., Wen C.: Int. J. Electrochem. Sci., 2015, **10**, 3767.
- [13] Zhang H., Han Z., Deng Q.: Nanomaterials, 2019, **9**, 694. <https://doi.org/10.3390/nano9050694>
- [14] Du H., Zhou C., Xie X. *et al.*: Int. J. Hydrogen Energy, 2017, **42**, 15236. <https://doi.org/10.1016/j.ijhydene.2017.04.109>
- [15] Hakamada M., Mabuchi M.: J. Alloys Comp., 2009, **485**, 583. <https://doi.org/10.1016/j.jallcom.2009.06.031>
- [16] Dan Z., Qin F., Sugawara Y. *et al.*: Intermetallics, 2012, **31**, 157. <https://doi.org/10.1016/j.intermet.2012.06.018>
- [17] Qiu H.-J., Kang J., Liu P. *et al.*: J. Power Sources, 2014, **247**, 896. <https://doi.org/10.1016/j.jpowsour.2013.08.070>
- [18] Wang L., Balk T.: Philosoph. Magazine Lett., 2014, **94**, 573. <https://doi.org/10.1080/09500839.2014.944600>
- [19] Sechi E., Vacca A., Mascia M. *et al.*: Chem. Eng. Transact., 2016, **47**, 97. <https://doi.org/10.3303/CET1647017>
- [20] Kuntiyi O., Ivashkin V., Yavorskii V. *et al.*: Russ. J. Appl. Chem., 2007, **80**, 1856. <https://doi.org/10.1134/S1070427207110158>
- [21] Kim S., Jung H.-D., Kang M.-H. *et al.*: Mater. Sci. Eng. C, 2013, **33**, 2808. <https://doi.org/10.1016/j.msec.2013.03.011>
- [22] Panagiotopoulos N., Jorge A., Rebai I. *et al.*: Micropor. Mesopor. Mater., 2016, **222**, 23. <https://doi.org/10.1016/j.micromeso.2015.09.054>
- [23] Zhang F., Li P., Yu J. *et al.*: J. Mater. Res., 2017, **32**, 1528. <https://doi.org/10.1557/jmr.2017.19>
- [24] Erlebacher J., Aziz M., Karma A.: Nature, 2001, **410**, 450. <https://doi.org/10.1038/35068529>
- [25] Zhao W., Liu N., Rong J. *et al.*: Adv. Eng. Mater., 2017, **19**, 1600866. <https://doi.org/10.1002/adem.201600866>
- [26] Saldan I.: J. Solid State Electrochem., 2010, **14**, 1339. <https://doi.org/10.1007/s10008-009-0974-3>
- [27] Saldan I., Burtovyy R., Becker H.W. *et al.*: Int. J. Hydrogen Energy, 2008, **33**, 7177. <https://doi.org/10.1016/j.ijhydene.2008.09.002>
- [28] Saldan I.: Int. J. Hydrogen Energy, 2016, **41**, 11201. <https://doi.org/10.1016/j.ijhydene.2016.05.062>
- [29] Gosalawit-Utke R., Nielsen T. K., Saldan I. *et al.*: J. Phys. Chem. C, 2011, **115**, 10903. <https://doi.org/10.1021/jp2021903>
- [30] Miettinen J.: Calphad, 2005, **29**, 40. <https://doi.org/10.1016/j.calphad.2005.02.002>
- [31] Wang H., Reed R., Gebelin J. *et al.*: Calphad, 2012, **39**, 21. <https://doi.org/10.1016/j.calphad.2012.06.007>
- [32] Saldan I., Frenzel J., Shekhah O. *et al.*: J. Alloys Compd., 2009, **470**, 568. <https://doi.org/10.1016/j.jallcom.2008.03.050>

Received: November 22, 2019 / Revised: December 24, 2019 /
Accepted: February 02, 2020

ХІМІЧНЕ ВИЛУГОВУВАННЯ ЗА КІМНАТНОЇ ТЕМПЕРАТУРИ СПЛАВІВ Al_3Ni ТА Al_3Ti

Анотація. Методом дугової плавки приготовлені Al_3Ni та Al_3Ti сплави і витримані у 5M NaOH для хімічного вилугування за кімнатної температури. Встановлено, що у випадку Al_3Ni сплаву збагачені алюмінієм фази реагують з розчином вилугування з утворенням нанопористого нікелю з діаметром пор у діапазоні ~10–20 нм. Доведено, що тільки фаза чистого алюмінію сплаву Al_3Ti реагувала хімічно з утворенням густоскладчастої поверхні з розміром складки ~50–100 нм.

Ключові слова: нікель, титан, пористий матеріал, X-променева дифракція, морфологія поверхні.